



Theoretical And Practical Analysis Of Dry Friction Processes In Mechanical Systems

Yusupov Alijon Abdujabbor ugli

PhD Assistant, Department of Mechanics, Namangan State Technical University, Namangan, Uzbekistan

E-mail: alijonyusupov533@gmail.com

Abdurahmonov Jahongir Bahodir ugli

PhD Assistant, Department of Mechanics, Namangan State Technical University, Namangan, Uzbekistan

E-mail: jahongirabdurahmonov09@gmail.com

Abstract

Dry friction is an essential component of mechanical systems and represents the resisting force that arises between bodies in the absence of a lubricating medium. This topic analyzes the theoretical foundations of dry friction, in particular the Amontons–Coulomb laws and their limitations of applicability. The dependence of the friction coefficient on material properties, surface roughness, and external conditions is studied. In addition, the differences between static and kinetic friction and their influence on the stability of mechanical systems are examined. From a practical perspective, the role of dry friction in machines and mechanisms, as well as its effects on energy losses and wear processes, is analyzed. The results of the study are important for improving the efficiency of mechanical systems and extending their service life. Furthermore, modern modeling methods are discussed as a means of achieving a more accurate representation of friction phenomena. This topic is considered highly relevant for the fields of mechanics and engineering.

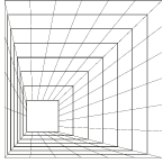
Keywords: dry friction, friction force, static friction, kinetic friction, friction coefficient, surface roughness, wear process, energy losses, mechanical systems, Amontons–Coulomb laws, tribology, modeling methods.

Introduction

Dry friction is regarded as one of the most important classical problems in the fields of tribology and contact mechanics. Early fundamental studies have shown that the frictional force depends not on the nominal contact area, but rather on the real area of contact between interacting surfaces. In the classical works of Bowden and Tabor, it was demonstrated that the real contact area between two solid surfaces is significantly smaller than the apparent (nominal) contact area, and that friction arises specifically through micro-contacts at asperity junctions [1]. Later, Greenwood and Williamson described the contact of rough surfaces using a statistical asperity model, which advanced the understanding of the real contact problem between nominally flat surfaces to a new scientific level [2].

Thus, a review of the existing literature allows the identification of five main scientific directions in the study of dry friction phenomena: the theory of real contact area [1], statistical models of asperities [2], multiscale surface roughness and spectral approaches [3], modern reviews based on contact mechanics [4–5], and experimental studies of the running-in process and tribochemical effects [6–7]. Therefore, dry friction should not be interpreted as a simple resistive force, but rather as a complex contact phenomenon governed by surface topography, material properties, adhesion, and environmental influences [1].

Characteristics of dry friction



Frictional force is defined as the force that resists motion when two surfaces in contact either slide relative to each other or tend to do so. This force always acts tangentially at the points of contact and is directed opposite to the actual or potential direction of motion. In this section, the phenomenon of dry friction is considered. Dry friction, also known as Coulomb friction, is so named because its fundamental characteristics were extensively studied by the French physicist Charles-Augustin de Coulomb in 1781. Dry friction occurs in the absence of lubricating fluids between contacting surfaces.



The heat generated as a result of abrasive (wear-by-rubbing) friction can be clearly observed during the sharpening of a metal blade using a grinding tool.

Another type of friction—fluid friction—is studied within the field of fluid mechanics.

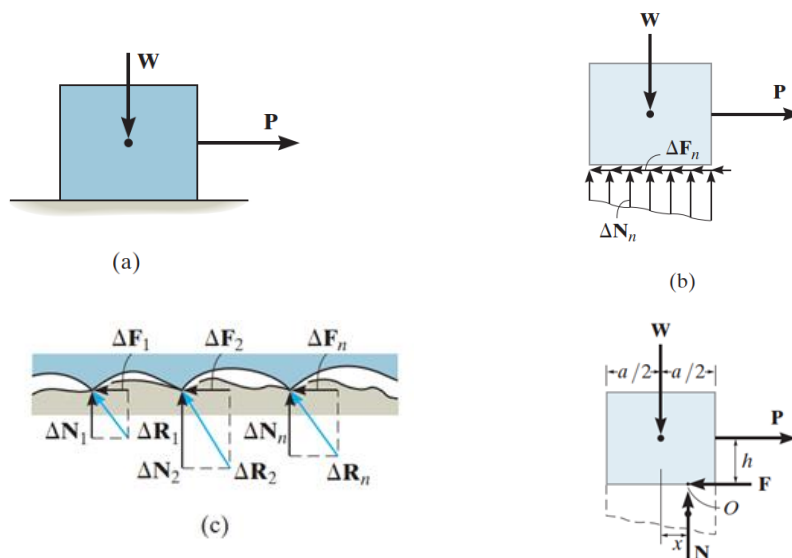


Figure 1. Schematic representation of dry friction and contact forces between rough surfaces

Theory of Dry Friction

The theory of dry friction can be explained as follows: a block of weight W , uniformly distributed, rests on a rough horizontal surface. The surface is not perfectly rigid and undergoes slight deformation (flexibility), as shown in Fig. 1a. However, the upper part of the block may be considered rigid. In the free-body diagram of the block, as illustrated in Fig. 1b, the floor exerts a non-uniformly distributed normal force ΔN_n and frictional force ΔF_n along the contact surface with the block.

For equilibrium, the normal forces must act upward to balance the weight W of the block. The frictional forces act to the left, since they prevent the applied force P from causing the block to slide to the right. By examining the contact surfaces between the floor and the block more



closely, the mechanism of generation of frictional and normal forces becomes evident, as shown in Fig. 1c. The interface between the two surfaces contains a large number of microscopic irregularities (asperities), and at each contact point, reaction forces ΔR_n are generated. It can be observed that each reaction force has two components: a frictional component ΔF_n and a normal component ΔN_n .

Equilibrium. The distributed effects of the normal and frictional forces along the contact surface can be represented in the free-body diagram by their resultant forces N and F , as shown in Fig. 1d. It should be noted that the normal force N is shifted by a distance x to the right relative to the line of action of the weight W , as shown in Fig. 1d. This position corresponds to the centroid (geometrical center) of the distribution of normal forces shown in Fig. 1b and is necessary to counteract the overturning effect produced by the force P . For example, if the force P is applied at a height h above the surface (Fig. 1d), then the moment equilibrium about point O is satisfied as follows:

$$Wx = Ph.$$

So,

$$x = Ph/W.$$

In addition to the mechanical interactions described above (commonly referred to as the classical approach), a more detailed analysis of the nature of frictional forces must also take into account the influence of factors such as temperature at the contacting surfaces, material density, surface cleanliness, as well as atomic or intermolecular attractive forces.

When the block is on the verge of sliding, the normal force N and the limiting static friction force F_s combine to form a resultant force R_s , as shown in Fig. 1e. The angle ϕ_s formed between R_s and N is referred to as the angle of static friction. According to Fig. 1,

$$\phi_s = \tan^{-1} \left(\frac{F_s}{N} \right) = \tan^{-1} \left(\frac{\mu_s N}{N} \right) = \tan^{-1} \mu_s \quad (1)$$

Typical values for the coefficient of static friction (μ_s) are systematically presented in Table 1 for comparative analysis. It is imperative to acknowledge that these empirical values are subject to potential variations, primarily because experimental assessments are conducted under diverse conditions involving:

- The specific degree of surface roughness and micro-topography;
- The level of surface cleanliness and presence of contaminants;
- The environmental factors influencing the contacting materials;
- The precise mechanical properties of the interface.

Consequently, within the scope of practical engineering applications, it is of paramount importance to exercise professional engineering judgement and a high degree of caution when selecting the most appropriate friction coefficient for any given set of specific operating conditions. This ensures the structural integrity and functional reliability of the mechanical system under investigation.

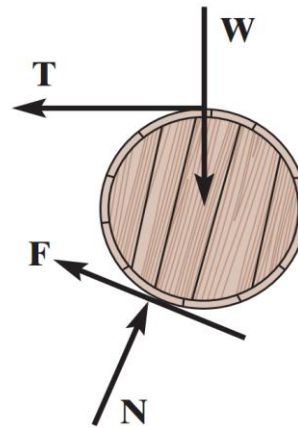
If a more accurate determination of F_s is required, the friction coefficient should be obtained directly through experimental testing involving the specific pair of materials under consideration.

Table 1. Typical values of the coefficient of friction

Interacting Contacting Materials	Coefficient of Static Friction, μ_s
Metal on ice	0.03-0.05
Wood on wood	0.30-0.70



Leather on wood	0.20-0.50
Leather on metal	0.30-0.60
Copper on copper	0.74-1.21



Some bodies, such as the barrel shown in the example, may not be in a state of impending slip; that is, they are not on the verge of sliding. Therefore, the frictional force F cannot be determined using the limiting condition

$$F = \mu_s N$$

Instead, it must be determined directly from the equations of static equilibrium.

Motion. If the magnitude of the applied force P acting on the block is increased so that it becomes slightly greater than the maximum static friction force F_s , the frictional force at the contact surface decreases to a lower value, F_k . This force is known as the kinetic, or sliding, friction force.

At this stage, the block begins to slide and its velocity increases, as shown in Fig. 2a. During sliding, the block effectively moves over the microscopic asperity peaks at the contact surface, as illustrated in Fig. 2b. The continuous deformation and wear of these surface asperities are considered the main mechanisms responsible for the generation of kinetic friction.

Experiments conducted on sliding blocks show that the magnitude of the kinetic friction force is directly proportional to the magnitude of the resultant normal force. Mathematically, this relationship is expressed as:

$$F_k = \mu_k N \tag{2}$$

Where F_k is the kinetic friction force, N is the resultant normal force, and μ_k is the coefficient of kinetic friction.

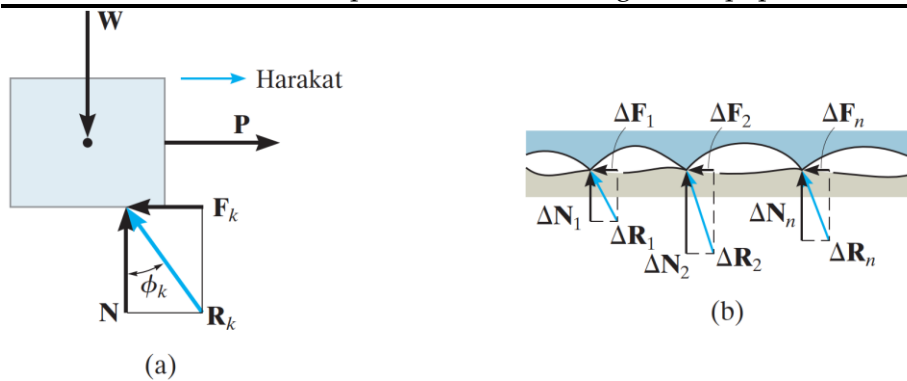


Figure 2. Kinetic friction mechanism during sliding motion: (a) free-body diagram of a sliding block; (b) microscopic contact between surface asperities.

Here, the constant of proportionality μ_k is called the coefficient of kinetic friction. The typical values of μ_k are approximately 25 percent lower than the values of μ_s given in Table 1.

As shown in Fig. 2a, in this case the line of action of the resultant force R_k generated at the contact surface is defined by the angle ϕ_k . This angle is called the angle of kinetic friction and is defined as follows:

$$\phi_k = \tan^{-1} \left(\frac{F_k}{N} \right) = \tan^{-1} \left(\frac{\mu_k N}{N} \right) = \tan^{-1} \mu_k \quad (3)$$

Compared to, $\phi_s \geq \phi_k$.

The friction-related effects described above can be summarized using the graph shown in Fig. 3. The graph illustrates how the frictional force F varies as a function of the applied (external) load P . In this representation, the frictional force is classified into three different forms:

- If the body remains in equilibrium (i.e., no sliding occurs), F is the static friction force.
- If the frictional force reaches its maximum value required to maintain equilibrium, this value is called the limiting (maximum) static friction force F_s .
- If sliding occurs at the contact surfaces, F becomes the kinetic (sliding) friction force F_k .

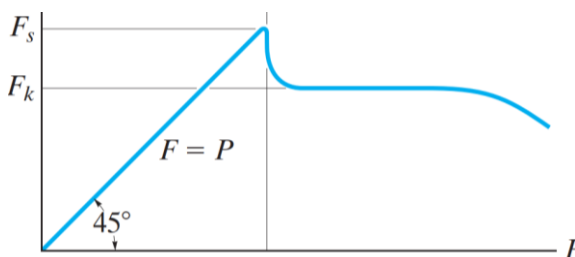
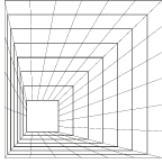


Fig 3. Graph of the dependence of frictional force on the applied force.

From the graph it can also be observed that when P becomes very large or when the velocity is high, aerodynamic effects begin to reduce F_k , and consequently the kinetic friction coefficient μ_k also starts to decrease.

Problems involving dry friction. If a rigid body is in equilibrium under the action of a system of forces that includes friction, the system must satisfy not only the equilibrium equations but also the laws governing frictional forces.

No indication of sliding motion. Problems of this type are pure equilibrium problems, in which



the number of unknowns must be equal to the number of available equilibrium equations. However, after solving for the frictional forces, their numerical values must be verified: they must satisfy the inequality $F \leq \mu_s N$; otherwise, sliding will occur and the body will not remain in equilibrium. An example of this type of problem is shown in Fig. 4a. Here, to check whether the equilibrium of a two-member frame can be maintained, it is necessary to determine the frictional forces at points A and C. If the rods are uniform and each has a weight of 100 N, then the free-body diagrams are as shown in Fig. 4b.

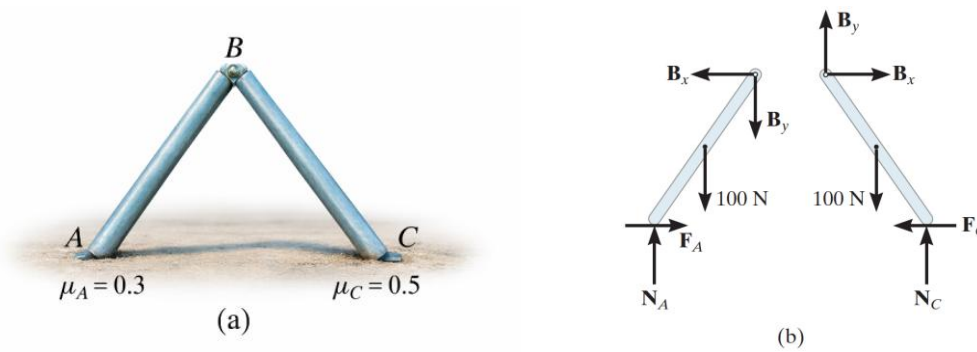


Fig. 4. Free-body diagrams of a two-rod system with frictional contact at points A and C.

In this case, there are six unknown force components, which can be determined strictly from six equilibrium equations (three for each rod). After determining F_A, N_A, F_C , and N_C the following conditions must be satisfied in order for the rods to remain in equilibrium: $F_A \leq 0.3N_A$ and $F_C \leq 0.5N_C$

Impending motion at all contact points (incipient sliding). In this case, the total number of unknowns is equal to the sum of the number of available equilibrium equations and the number of friction equations of the form $(F = \mu N)$. When motion at the contact points is about to begin, limiting static friction is given by $F_s = \mu_s N$; if the body is already sliding, kinetic friction is expressed as $F_k = \mu_k N$.

As an example, consider the problem shown in Fig. 5a, where a 100 N rod rests against a wall without slipping. The task is to determine the minimum angle at which the rod can be placed while maintaining equilibrium. The free-body diagram is shown in Fig. 5b.

In this case, there are five unknowns, which are determined using three equilibrium equations together with two friction equations applied at the contact points, namely $F_A = 0.3N_A$ and $F_B = 0.4N_B$.

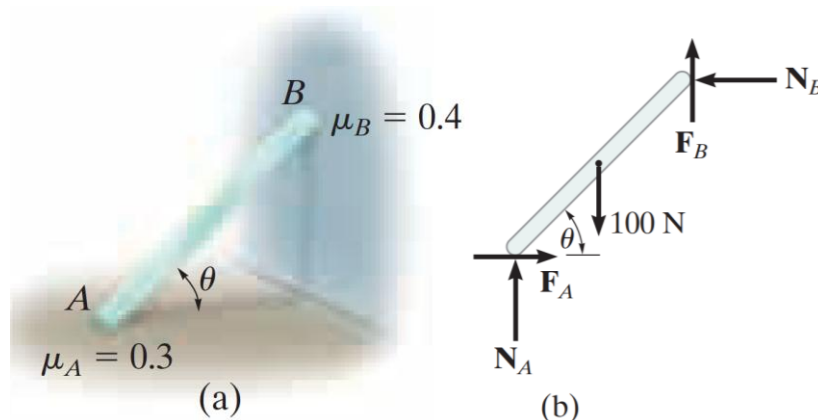
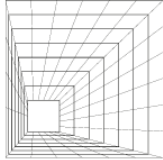


Fig. 5. Free-body diagram of a rod in impending sliding contact with a rough floor and wall.



Problem 1. The mass of the homogeneous box shown in Fig. 6a is 20 kg. When a force $P = 80 \text{ N}$ is applied to the box, determine whether it remains in equilibrium or not. The coefficient of static friction is given as $\mu_s = 0.3$.

Solution. Free-body diagram. As shown in Fig. 6b, the resultant normal reaction force N_C must act at a distance x from the central axis of the box. This position is necessary to balance the overturning moment produced by the force P .

In this problem, there are three unknowns: F , N_C , and x . All of them can be determined directly using the three equilibrium equations.

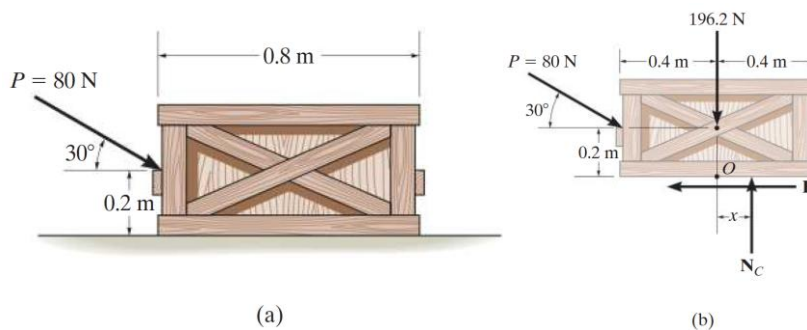


Fig. 6. Equilibrium equations:

$$\begin{aligned} \sum F_x = 0; & \quad 80 \cos 30^\circ - F = 0 \\ \sum F_y = 0; & \quad -80 \sin 30^\circ + N_C - 196.2 = 0 \\ \sum M_O = 0; & \quad 80 \sin 30^\circ (0.4) - 80 \cos 30^\circ (0.2) + N_C(x) = 0 \end{aligned}$$

Based on the solution of the equations:

$$F = 69.3 \text{ N}; \quad N_C = 236.2 \text{ N}; \quad x = 0.00908 \text{ m} = -9.08 \text{ mm}$$

Since the obtained value of x is negative, the resultant normal force acts slightly to the left of the central axis of the box. However, since $|x| < 0.4 \text{ m}$, the line of action of the normal force still lies within the base of the box. Therefore, overturning does not occur.

The maximum available friction force at the contact surface is:

$$F_{\max} = \mu_s N_C = 0.3(236.2 \text{ N}) = 70.9 \text{ N}. \quad (4)$$

Also, the maximum possible friction force at the contact surface is

$F_{\max} = \mu_s N_C = 0.3(236.2 \text{ N}) = 70.9 \text{ N}$ Since $F = 69.3 \text{ N} < 70.9 \text{ N}$, the box does not slide, although it is very close to the slipping condition.

Problem 2. It was observed that vending machines begin to slide off the surface of a truck bed when the bed is tilted to an angle of $\theta = 25^\circ$, as shown in Fig. 8.8a. Determine the coefficient of static friction between the vending machine and the surface of the truck bed.

Solution: The simplified model of the vending machine placed on the truck bed is shown in Fig. 7b. Its dimensions have been measured and the center of gravity has been determined. The weight of the vending machine is taken as W .

Free-body diagram. As shown in Fig. 7c, the distance x is introduced to locate the point of application of the resultant normal force N . In this problem, there are four unknowns: N , F , μ_s etc.

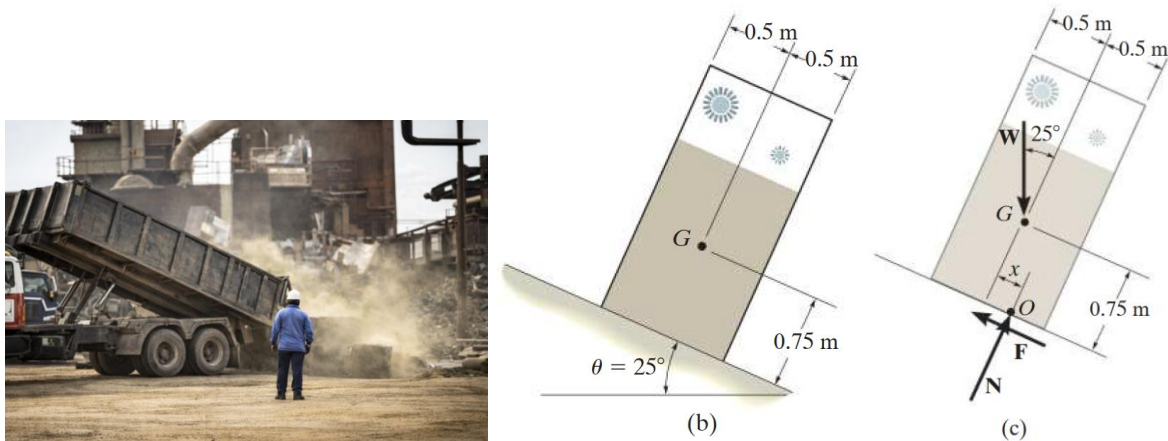
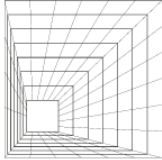


Fig. 7.

Equilibrium equations:

$$+\square \sum F_x = 0; \quad W \sin 25^\circ - F = 0 \tag{5}$$

$$+\square \sum F_y = 0; \quad N - W \cos 25^\circ = 0 \tag{6}$$

$$\tilde{N} + \sum M_o = 0; \quad - W \sin 25^\circ (0.75m) + W \cos 25^\circ (x) = 0 \tag{7}$$

$\theta = 25^\circ$ Since the system is on the verge of sliding, equations (1) and (2) can be used to obtain the following result:

$$F_s = \mu_s N; \quad W \sin 25^\circ = \mu_s (W \cos 25^\circ)$$

$$\mu_s = \tan 25^\circ = 0.466$$

$\theta = 25^\circ$ This angle is called the limiting equilibrium angle, also known as the natural angle of repose. From comparison, it is found that this angle is equal to the angle of static friction, i.e., $\theta = \phi_s$. From the calculations, it can be seen that the angle θ does not depend on the weight of the vending machine. Therefore, knowing the angle θ provides a convenient method for determining the coefficient of static friction.

Note: From equation (3), it is found that $x \approx 0.34 \text{ m}$. $0.34 \text{ m} < 0.5 \text{ m}$. Since, the vending machine begins to slide before overturning, as observed in Fig. 7a.

Problem 3. The masses of blocks (A) and (B) are 3 kg and 9 kg, respectively. They are connected by weightless rods, as shown in Fig. 8a. Determine the maximum vertical force (P) that can be applied at the hinge point (C), provided that no motion occurs in the system. The coefficient of static friction between the blocks and their contacting surfaces is:

Solution. Free-body diagram. The rods are two-force members; therefore, the free-body diagrams of the hinge point C and blocks A and B are shown in Fig. 7b.

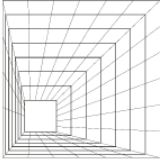
Since the horizontal component of the force F_{AC} tends to move block A to the left, the friction force F_A must act to the right in order to oppose this motion. Similarly, because the force F_{BC} tends to move block B to the right, the friction force F_B acts to the left to resist this motion.

The system contains seven unknowns, while there are six equilibrium equations available (two for the hinge C and two for each block A and B). Therefore, only one additional friction condition is required.

Conclusion

In this work, the phenomenon of dry friction was systematically studied within mechanical systems as a multiparameter contact process. The results show that the formation of frictional force is closely related to the real contact area, surface topography, the physical and mechanical properties of materials, as well as adhesion and tribochemical effects.

Although the classical Amontons–Coulomb laws play an important role in engineering



calculations, they are often idealized models and cannot fully represent complex real conditions. The analysis of static and kinetic friction regimes confirms their significant influence on the stability of mechanical systems, energy dissipation, and wear processes. In particular, the onset of sliding and the variability of the friction coefficient are of great importance in practical applications.

Furthermore, modern approaches in contact mechanics and modeling provide more accurate descriptions of dry friction phenomena. As a result, the deep and comprehensive study of dry friction serves as an essential scientific basis for optimizing mechanical systems, reducing energy losses, and increasing the service life of engineering structures.

References

1. Bobojanov, H. T., & Yusupov, A. A. O'g'li. (2020). Change of physical and mechanical properties of twisted yarn during rewinding. *The American Journal of Engineering and Technology*, 2(08), 64–69. <https://doi.org/10.37547/tajet/Volume02Issue08-09>
2. Bowden, F. P., & Tabor, D. (1939). The area of contact between stationary and moving surfaces. *Proceedings of the Royal Society of London. Series A. Mathematical and Physical Sciences*, 169(938), 391–413.
3. Ghatrehsamani, S., Akbarzadeh, S., & Khonsari, M. M. (2022). Experimentally verified prediction of friction coefficient and wear rate during running-in dry contact. *Tribology International*, 170, Article 107508. <https://doi.org/10.1016/j.triboint.2022.107508>
4. Greenwood, J. A., & Williamson, J. B. P. (1966). Contact of nominally flat surfaces. *Proceedings of the Royal Society of London. Series A. Mathematical and Physical Sciences*, 295(1442), 300–319.
5. Huang, S., Zhang, S., Wei, D., Song, H., et al. (2025). Frictional strength regulated by roughness alignment. *Science Advances*, 11(38), Article eady6779. <https://doi.org/10.1126/sciadv.ady6779>
6. Persson, B. N. J., Albohr, O., Tartaglino, U., Volokitin, A. I., & Tosatti, E. (2005). On the nature of surface roughness with application to contact mechanics, sealing, rubber friction and adhesion. *Journal of Physics: Condensed Matter*, 17(1), R1–R62.
7. Popov, V. L., Li, Q., & Lyashenko, I. A. (2025). Contact mechanics and friction: Role of adhesion. *Friction*, 13(1), Article 9440964. <https://doi.org/10.26599/FRICT.2025.9440964>
8. Yuldashev, J. Q., & Bobojanov, H. T. (2020). Study of the influence of the parameters of the sampling zone on the condition of the capture of fibers by the drum teeth. *The American Journal of Engineering and Technology*, 2(08), 75–78. <https://doi.org/10.37547/tajet/Volume02Issue08-11>
9. Yusupov, A., Bobojanov, H., Yusupov, S., & Yuldasheva, G. (2025). Calculation theory of yarns under the influence of a grooved cylinder on a ring spinning machine. *AIP Conference Proceedings*, 3304(1), Article 030086.
10. Zhang, S., Li, D., & Liu, Y. (2022). Friction behavior of rough surfaces on the basis of contact mechanics: A review and prospects. *Micromachines*, 13(11), Article 1907. <https://doi.org/10.3390/mi13111907>